Binding of Daunomycin to Diaminopurine- and/or Inosine-Substituted DNA[†,‡]

Christian Bailly,[§] Dongchul Suh,[||] Michael J. Waring,[⊥] and Jonathan B. Chaires*[,||]

Laboratoire de Pharmacologie Antitumorale Moléculaire du Centre Oscar Lambret et INSERM U-124, Place de Verdun, 59045 Lille, France, Department of Pharmacology, University of Cambridge, Tennis Court Road, Cambridge CB2 1QJ, U.K., and Department of Biochemistry, University of Mississippi Medical Center, 2500 North State Street, Jackson, Mississippi 39216-4505

Received July 3, 1997; Revised Manuscript Received September 24, 1997

ABSTRACT: The binding of the anticancer drug daunomycin to double-helical DNA has been investigated by DNase I footprinting and fluorescence titration, using a series of polymerase chain reaction (PCR) synthesized DNA fragments that contained systematic base substitutions to alter the disposition of functional groups within the minor groove. The 160 bp *tyrT* DNA fragment constituted the starting material. Fragments in which (i) inosine was substituted for guanosine, (ii) diaminopurine was substituted for adenine, and (iii) both inosine and diaminopurine were substituted for guanosine and adenine, respectively, were studied. These fragments permit the role of the 2-amino group in the minor groove to be systematically explored. The results of DNase I footprinting experiments confirmed that daunomycin binds preferentially to 5′(A/T)GC and 5′(A/T)CG triplets in the normal fragment. Substitution of inosine for guanosine, with the concomitant loss of the N-2 in the minor groove, weakened binding affinity but did not dramatically alter the sequence preference associated with daunomycin binding. Complete reversal of the location of the N-2 group by the double substitution, however, completely altered the sequence preference of daunomycin and shifted its binding from the canonical triplets to ones with a 5′IDD motif. These results have critically tested and confirmed the proposed key roles of the daunosamine moiety and the 9-OH group of daunomycin in dictating binding to preferred sites. In a parallel study, both macroscopic and microscopic binding to the normal *tyrT* fragment were investigated, experiments made possible by using PCR to prepare large quantities of the long, defined DNA sequence. The results of these experiments underscored the complexity of the interaction of the drug with the DNA lattice and revealed unequivocal heterogeneity in its affinity for different binding sites. A class of high-affinity sites, most probably corresponding to the 5′(A/T)GC and 5′(A/T)CG triplets, was identified and characterized in macroscopic binding isotherms.

Anthracycline antibiotics are among the most potent weapons in the chemical arsenal used for cancer chemotherapy. After more than three decades in the clinic daunomycin (daunorubicin) and adriamycin (doxorubicin), the prototype anthracycline antibiotics, remain among the most frequently used antitumor drugs. Adriamycin, in particular, has the widest spectrum of activity against human cancers of any agent in current use (*1*).

The structure of daunomycin (Figure 1) can be divided into three functional domains: (i) the planar anthraquinone ring system, which intercalates into DNA; (ii) the puckered anchor D ring, which provides additional contacts with DNA via direct and indirect (solvent-mediated) hydrogen-bonding interactions; and (iii) the daunosamine sugar, which acts as a minor groove binder and is essential for the recognition of the DNA base surface within the helical groove. This positively charged carbohydrate moiety provides favorable polyelectrolyte contributions to the binding free energy, as well as additional sequence-dependent interactions between its amine group and DNA (see ref *2* for a recent review). Footprinting studies have demonstrated that daunomycin preferentially recognizes the triplet motifs 5′-(A/T)CG and 5′-(A/T)GC (*3*, *4*). Among the several hydrogen-bonding interactions that stabilize daunomycin−DNA complexes, a bifurcated H-bond between the C-9 hydroxyl of the drug and the N-3 and the exocyclic amino group of the guanine at the center of the preferred triplet binding site seems to be crucial for the stability of the complex. For this reason, and also because it is involved in controlling the width of the minor groove (*5*), it may be expected that the 2-amino group of guanine would modulate the recognition of defined DNA sequences by daunomycin.

We therefore set out to analyze the effect of adding, deleting, or relocating the 2-amino group of guanine on the binding of daunomycin to DNA. The effect of such modifications on the recognition of (A/T)GC or (T/A)CG triplets by daunomycin was examined. The modifications

[†] This work was done under the support of research grants (to C.B.) from the Association pour la Recherche sur le Cancer, (to M.J.W.) from the Wellcome Trust, CRC, AICR, and the Sir Halley Stewart Trust, and (to J.B.C.) CA35635 from the National Cancer Institute.

[‡] This paper is dedicated to the memory of Professor Bernard Pullman, who profoundly influenced our views of drug−DNA binding reactions and provided much inspiration and insight.

* Address correspondence to this author.

[§] COL−INSERM U124.

[||] University of Mississippi Medical Center.

[⊥] University of Cambridge.

S0006-2960(97)01612-7 CCC: $15.00
Published on Web 01/07/1998

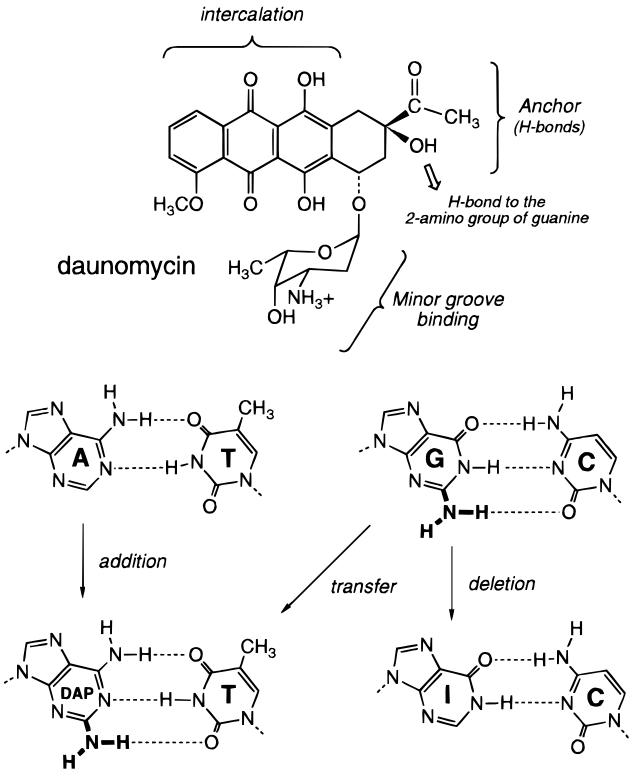

FIGURE 1: (top) Structure of daunomycin. The functional domains important for DNA binding are emphasized. (Bottom) Structures of hydrogen-bonded purine−pyrimidine base pairs. Broken lines represent hydrogen bonds. I represents inosine; DAP represents 2,6-diaminopurine (2-aminoadenine). The purine 2-amino group is shown in boldface type.

were incorporated into PCR-made DNA fragments using mixtures of natural bases and 2,6-diaminopurine (DAP) or inosine (I) or both I and DAP (Figure 1). Such a structural perturbation strategy has proved to be a powerful approach for probing the thermodynamics of site-specific protein−DNA interactions (*6*, *7*). The use of PCR allows us to make long chemically modified DNA fragments for study, in contrast to the shorter modified oligonucleotides prepared by direct synthesis used in protein−DNA interaction studies (*6*, *7*).

In a separate aspect of this work, a combination of fluorescence titrations experiments and DNase I footprinting was used to measure, for the first time in a homogeneous DNA fragment, both macroscopic and microscopic drug binding events. These studies have revealed the underlying complexity of drug binding to a DNA lattice of defined sequence and challenge the fundamental assumptions made in the neighbor exclusion model commonly used to analyze drug−DNA interactions.

By carefully investigating the well-characterized and clinically useful antibiotic daunomycin, we have gleaned fundamental information that furnishes a better understanding of the rules that govern drug−DNA recognition.

MATERIALS AND METHODS

Chemicals and Biochemicals. Daunomycin (Sigma Chemical Co.) was first dissolved in water to yield a 1 mM stock solution. Subsequent dilutions of the drug were made with 10 mM Tris and 10 mM NaCl buffer, adjusted to pH 7.0. The drug concentration was determined photometrically applying a molar extinction coefficient of 11 500 M^{-1} cm^{-1} at 477 nm. Ammonium persulfate, tris base, acrylamide, bisacrylamide, ultrapure urea, boric acid, tetramethylethylenediamine, and dimethylsulfate were from BDH. Formic acid, piperidine, and formamide were from Aldrich. Bromophenol blue and xylene cyanol were from Serva. The nucleoside triphosphate labeled with [γ-^{32}P]ATP) was obtained from NEN Dupont. Restriction endonucleases *Eco*RI and *Ava*I (Boehringer), *Taq* polymerase (Promega), DNase I (Sigma), and T4 polynucleotide kinase (Pharmacia) were used according to the supplier's recommended protocol in the activity buffer provided. The primers, 5′-AATTCCG-GTTACCTTTAATC and 5′-TCGGGAACCCCCAC-CACGGG, having a 5′-OH or 5′-NH_2 terminal group, were obtained from the Laboratory of Molecular Biology, Medical Research Council, Cambridge, England. Checks were carried out to ensure that the primers blocked with a 5′-NH_2 group were free from contaminants and not labeled by the kinase. All other chemicals were analytical-grade reagents, and all solutions were prepared using doubly deionized, Millipore filtered water.

Preparation, Purification, and Labeling of DNA Fragments Containing Natural and Modified Nucleotides. Plasmid pKMp27 (*8*) was isolated from *Escherichia coli* by a standard sodium dodecyl sulfate−sodium hydroxide lysis procedure and purified by banding in CsCl−ethidium bromide gradients. Ethidium was removed by several 2-propanol extractions followed by exhaustive dialysis against Tris−EDTA buffer. The purified plasmid was then precipitated and resuspended in appropriate buffer prior to digestion by the restriction enzymes. The 160 base pair *tyrT*(A93) fragment used as a template was isolated from the plasmid by digestion with restriction enzymes *Eco*RI and *Ava*I. It is worth mentioning that this template DNA bore a 5′-phosphate due to the action of *Eco*RI and thus only the newly synthesized DNA (with normal or modified nucleotides) can be labeled by the kinase.

Polymerase Chain Reaction. The protocol used to incorporate inosine and/or 2,6-diaminopurine residues into DNA is comparable to those previously used to incorporate 7-deazapurine or inosine residues with only a few minor modifications (*9*, *10*). PCR reaction mixtures contained 10 ng of *tyrT*(A93) template, 1 mM each of the appropriate pair of primers (one with a 5′-OH and one with a 5′-NH_2 terminal group) required to allow 5′-phosphorylation of the desired strand, 250 mM of each appropriate dNTP (dTTP, dCTP plus dATP or dDTP and dGTP or dITP according to the desired DNA), and 5 units of *Taq* polymerase in a volume of 50 mL containing 50 mM KCl, 10 mM Tris-HCl, pH 8.3, 0.1% Triton X-100, and 1.5 mM $MgCl_2$. To prevent unwanted primer−template annealing before the cycles began, the reactions were heated to 60 °C before addition of *Taq* polymerase (*11*). Finally, paraffin oil was added to each reaction to prevent evaporation. After an initial denaturing step of 3 min at 94 °C, 20 amplification cycles were performed, with each cycle consisting of the following segments: 94 °C for 1 min, 37 °C for 2 min, and 72 °C for 10 min. After the last cycle, the extension segment was continued for an additional 10 min at 72 °C, followed by a 5 min segment at 55 °C and a 5 min segment at 37 °C. The purpose of these final segments was to maximize annealing

of full-length product and to minimize annealing of unused primer to full-length product. The reaction mixtures were then extracted with chloroform to remove the paraffin oil, and parallel reactions were pooled. Several extractions with water-saturated *n*-butanol were performed to reduce the volume prior to loading of the samples onto a 6% nondenaturing polyacrylamide gel. After electrophoresis for about 1 h, a thin section of the gel was stained with ethidium bromide so as to locate the band of DNA under UV light. The same band of DNA free of ethidium was excised, crushed, and soaked in elution buffer (500 mM ammonium acetate, 10 mM magnesium acetate) overnight at 37 °C. This suspension was filtered through a Millipore 0.22 mm filter and the DNA was precipitated with ethanol. Following washing with 70% ethanol and vacuum-drying of the precipitate, the purified DNA was resuspended in the kinase buffer.

DNA Labeling and Purification. The purified PCR products were 5′-end-labeled with [γ-^{32}P]ATP in the presence of T4 polynucleotide kinase according to a standard procedure for labeling blunt-ended DNA fragments (*12*). After completion, the labeled DNA was again purified by 6% polyacrylamide gel electrophoresis and extracted from the gel as described above. Finally, the labeled DNA was resuspended in 10 mM Tris-HCl buffer, pH 7.0, containing 10 mM NaCl.

DNase I Footprinting. DNase I experiments were performed as previously described (*13*). The digestion of the samples (6 μL) of the labeled DNA fragment dissolved in 10 mM Tris buffer, pH 7.0, containing 10 mM NaCl was initiated by the addition of 2 μL of a DNase I solution whose concentration was adjusted to yield a final enzyme concentration of about 0.01 unit/mL in the reaction mixture. The extent of digestion was limited to less than 30% of the starting material so as to minimize the incidence of multiple cuts in any strand ("single-hit" kinetic conditions). Optimal enzyme dilutions were established in preliminary calibration experiments. After 3 min, the digestion was stopped by freeze-drying and the samples were lyophilized, washed once with 50 μL of water, lyophilized again, and then resuspended in 4 μL of an 80% formamide solution containing tracking dyes. Samples were heated at 90 °C for 4 min and chilled in ice for 4 min prior to electrophoresis.

Electrophoresis and Autoradiography. DNA cleavage products were resolved by polyacrylamide gel electrophoresis under denaturing conditions (0.3 mm thick, 8% acrylamide containing 8 M urea) capable of resolving DNA fragments differing in length by one nucleotide. Electrophoresis was continued until the bromophenol blue marker had run out of the gel (about 2.5 h at 60 W, 1600 V in TBE buffer, BRL sequencer model S2). Gels were soaked in 10% acetic acid for 15 min, transferred to Whatman 3MM paper, dried under vacuum at 80 °C, and subjected to autoradiography at −70 °C with an intensifying screen. Exposure times of the X-ray films (Fuji R-X) were adjusted according to the number of counts per lane loaded on each individual gel (usually 24 h).

Quantitation by Storage Phosphorimaging. A Molecular Dynamics 425E PhosphorImager was used to collect data from storage screens exposed to the dried gels overnight at room temperature (*14*). Baseline-corrected scans were analyzed by integrating all the densities between two selected boundaries using ImageQuant version 3.3 software. Each resolved band was assigned to a particular bond within the *tyrT*(A93) fragment by comparison of its position relative to sequencing standards generated by treatment of the DNA with formic acid followed by piperidine-induced cleavage at the purine residues (G + A track).

Data Reduction. Peak areas were stored on a disk as an ASCII file and subsequently transferred into standard spreadsheet programs (Cricket Graph and KaleidaGraph) using a Macintosh personal computer. The final data set consisted of 115 bands (positions 20−135) for each strand of the DNA fragment. At any given nucleotide position, data were measured for at least six daunomycin concentrations. Peak areas were determined in duplicate and were averaged. Over 3000 individual peak areas were thus examined in our analysis. The procedure used to derive footprinting plots was based on previous methods (*10*, *15*, *16*). In the first stage, peak areas were corrected for slight differences in the total amount of DNA loaded per lane by multiplying the peak area by a specific correction factor. This factor is determined from a total cut plot, i.e., a plot of the sum of all band intensities in a given lane vs the total daunomycin concentration. These individual corrections yield the "corrected" or "normalized" band intensities, which are used for quantitative comparison. In the present case, each total cut plot was a line of near-zero slope. Footprinting plots were then constructed by plotting R vs c, where c is the ligand concentration and the relative band intensity R corresponds to the ratio I_c/I_0, where I_c is the intensity of the band at a given concentration c and I_0 is the intensity of the same band in the control lane, i.e., in the absence of the antibiotic. The procedure employed to estimate the relative affinity of the antibiotic for defined sites consisted of using the first 4 or 5 concentrations in each footprinting plot and determining the initial slope by fitting them to a straight line and then dividing the slope of the line by the y-intercept. The more negative the slope, the higher the binding constant of the antibiotic at that site (*17*−*20*).

Fluorescence titration experiments were conducted with an ISS, Inc. (Champaign, IL) Greg 2000 photon-counting, steady-state fluorescence spectrometer. Excitation and emission wavelengths were set at 480 and 590 nm, respectively. Daunomycin was added to solutions containing the *tyrT*(A93) DNA fragment in 6 mM NaH_2PO_4, 2 mM Na_2HPO_4, 1 mM Na_2EDTA, and 185 mM NaCl in a volume of 0.5 mL. Separate titrations were made with solutions at DNA concentrations of 1, 5, and 10 μM (bp). Daunomycin was added to span a total added drug concentration of 0−3 μM, in 0.2 μM increments. The distribution of free and bound drug was calculated using

$$C_f = C_t(I/I_0 - P)/(1 - P)$$

where C_t and C_f are the total added and free drug concentrations, respectively, I is the measured fluorescence emission intensity in the presence of DNA, I_0 is the measured fluorescence emission intensity in buffer, and P is the ratio of quantum yields of the bound and free forms of the drug. P was determined in separate experiments to be 0.05 ± 0.01. The amount of bound daunomycin (C_b) was determined from

$$C_b = C_t - C_f$$

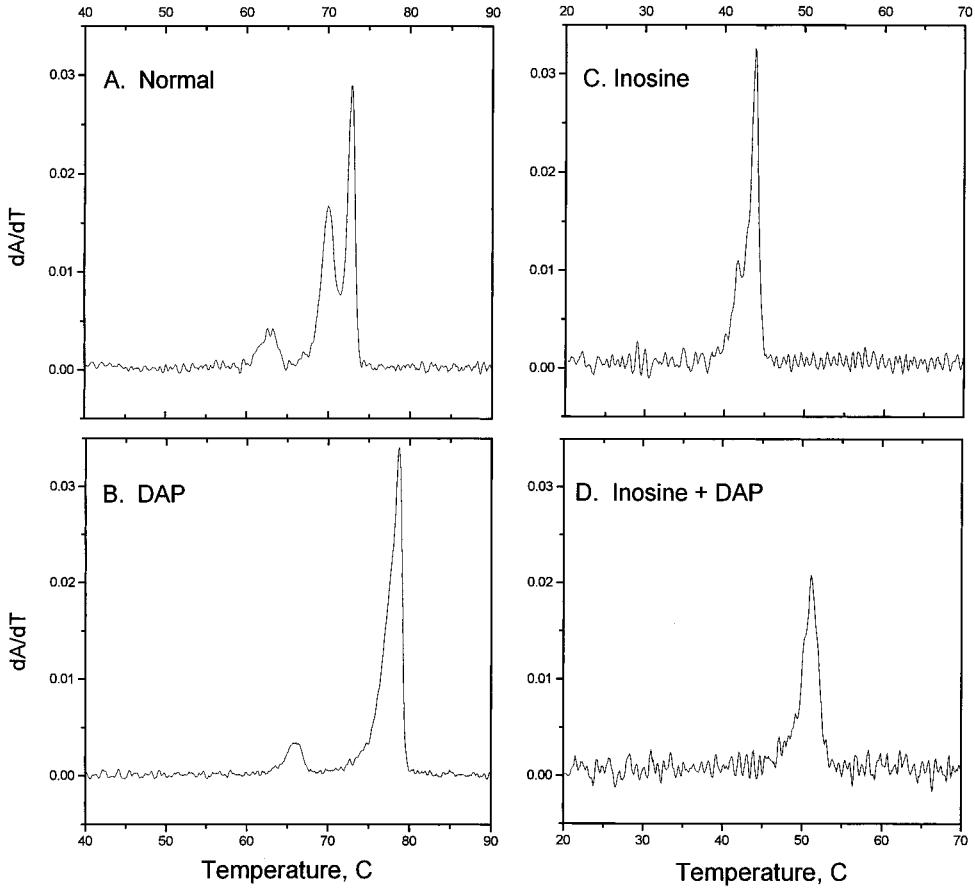

FIGURE 2: Differential melting curves for the normal *tyrT* DNA fragment (A) and fragments substituted with (B) diaminopurine, (C) inosine, or (D) inosine plus diaminopurine.

The binding ratio r was calculated in terms of DNA base pairs:

$$r = C_b/[\text{DNA}]$$

Quantitative Analysis of Binding Data. Nonlinear least-squares methods were used to fit binding data to various models, using fitting routines incorporated into FitAll (MTR Software, Toronto, Canada) and Origin (Microcal, Inc., Northampton, MA). Procedures and models for the analysis of drug−DNA binding isotherms have been fully described (*21*).

Circular Dichroism and UV Spectroscopy. All experiments were performed in BPE buffer consisting of 8 mM Na_2HPO_4 and 1 mM Na_2EDTA, titrated to pH 7.0. CD spectra were recorded on a Jasco J500 spectropolarimeter (Jasco, Inc., Easton, MD), interfaced to and controlled by an IBM personal computer. Spectra were recorded using 1 cm cylindrical cuvettes. Four spectra were recorded and averaged and corrected by subtraction of a buffer blank measured under identical conditions. Spectra are reported as $\Delta\epsilon = \epsilon_L - \epsilon_R$, that is, as the difference in the molar extinction coefficients for the absorbance of the left- (ϵ_L) or right- (ϵ_R) handed polarized light. $\Delta\epsilon$ is related to the molar ellipticity, $[\theta]$, by the relationship $[\theta] = 3300\Delta\epsilon$.

Absorption spectra were recorded using a Cary 3e spectrophotometer (Varian, Inc., Palo Alto, CA), as were UV melting profiles. For the latter, absorbance at 260 nm was monitored continuously while heating at a rate of 0.2 deg min^{-1}. Data were transferred to Origin (Microcal, Inc., Northampton, MA) for further analysis and graphic presentation. The UV absorption spectrum (not shown) of the unsubstituted *tyrT* DNA fragment was used to estimate the molar extinction coefficient at 260 nm using the method of Hirschman and Felsenfeld (*22*). The results yield $\epsilon_{260} = 12\,823$ $M(bp)^{-1}$ cm^{-1}. The estimate by that method is probably accurate to 10−15%.

RESULTS

The well-characterized *tyrT*(A93) fragment containing the *Escherichia coli tyrT* promoter was chosen as a substrate for both fluorescence and footprinting titration experiments. This DNA has been extensively used to study sequence-specific binding of drugs to DNA (*23*) and in particular was used in early experiments to demonstrate the selective binding of daunomycin to 5′-(A/T)CG and 5′-(A/T)GC triplet motifs (*3*, *4*).

Physical Properties of Normal and Substituted tyrT DNA. Figure 2 illustrates differential UV melting profiles for the *tyrT* fragments. Thermal denaturation of the unsubstituted, normal molecule reveals unanticipated complexity (Figure 2A). Three discrete transitions are evident, with T_m values of 62.7, 70.0 and 72.8 °C. Nondenaturing gel electrophoresis was used to verify that the fragment was homogeneous (not shown), so the complexity evident in the melting is not due to sample heterogeneity but rather is a property of the particular sequence. Substitution of the normal bases results in drastic alteration of the melting behavior of the fragment. In the PCR method used to synthesize fragments, modified bases are substituted into both strands of the DNA duplex.

Replacement of adenine with diaminopurine results in a marked thermal stabilization. T_m values of 65.9, 77.4, and 78.6 °C are observed after deconvolution of the melting profile shown in Figure 2B. Substitution of inosine for guanosine, by contrast, destabilizes the fragment and also reduces the complexity of the melting profile. T_m values of 42.4 and 43.8 °C are obtained from Figure 2C. Finally, substitution with both DAP and inosine produces a molecule that is significantly less stable than the normal one, with transitions at 49.5 and 51.2 °C (Figure 2D).

CD and UV difference spectra for the *tyrT* DNA fragment and its various substituted derivatives are shown in Supporting Information. All of the molecules studied have CD spectra characteristic of standard B-form DNA, although there are distinct differences apparent among the individual curves. Substituting diaminopurine for adenine produces a CD spectrum that differs most from that of the unsubstituted fragment. The maximum is shifted from ≈270 to 285 nm, and the positive lobe of the spectrum becomes distinctly biphasic with DAP present. The CD spectrum of the inosine-substituted fragment matches the curve for the normal fragment but shows less ellipticity at the minimum near 240 nm. The mixed substituted fragment, with both DAP and inosine, shows a spectrum intermediate between that of normal and DAP-substituted DNA.

UV difference spectra were determined for the substituted fragments (see Supporting Information) by normalizing their UV absorption spectra so as to match the absorbance of a solution of normal DNA at 260 nm. The difference between the spectra of the substituted and the normal fragments was then calculated. These difference spectra reveal certain subtle variations between the molecules containing normal bases and diaminopurine and inosine that would be expected to contribute to the CD spectra described above. For example, maximal absorbance differences in the DAP-substituted fragment are evident near 270 and 290 nm, in the same spectral region where the CD spectra of the normal and modified DNA fragments differ the most.

These physical studies establish that all the modified fragments remain in duplex form under the conditions of our experiments. There is little or no alteration of the global secondary structure of the substituted molecules; all of them appear to retain the standard B conformation. The effects of base substitution on daunomycin binding may therefore be attributed to local effects on the interaction.

Fluorescence Study of the Binding of Daunomycin to the tyrT Fragment. Figure 3A shows the binding isotherm, cast into the form of a Scatchard plot, for the interaction of daunomycin with the *tyrT*(A93) DNA fragment. Attempts to fit these data to the neighbor exclusion model of McGhee and von Hippel (*24*) were not successful. The best fit to the simple, two-parameter neighbor exclusion model

$$r/C_f = K(1 - nr)[(1 - nr)/(1 - (n - 1)r)]^{n-1}$$

where K is the binding constant and n is the exclusion parameter, is represented in Figure 3A. The fit yields values of $K = 3.7 \times 10^5$ M^{-1} and $n = 4.3$. There are, however, systematic deviations from the best-fit curve, indicating that this model is plainly an inadequate description of the experimental data. Attempts to fit the data to the extended McGhee−von Hippel neighbor exclusion model that includes an additional cooperativity parameter also proved unsuccessful (not shown). The experimental points exhibit more curvature than can be described even with the inclusion of a negative cooperativity term ($\omega < 1.0$). These calculations indicate that neighbor exclusion is an inappropriate description of the binding mechanism in this case and that the real situation must be more complicated than existing binding models allow.

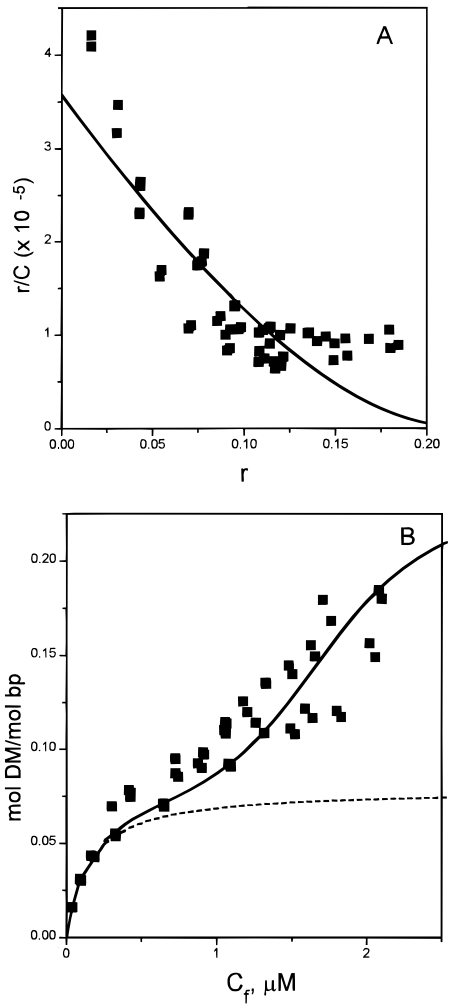

FIGURE 3: (A) Binding of daunomycin to the *tyrT* DNA fragment. Data are shown as a Scatchard plot. The best fit to the simple neighbor exclusion model is shown by the solid line, with the parameters described in the text. (B) Direct plot of daunomycin binding to the *tyrT* fragment. The isotherm was deconvoluted to evaluate the contribution of two classes of sites. The dashed line shows the best fit of the initial portion of the isotherm to a simple saturation function. The continuous line shows the composite curve resulting from the summation of the two classes of binding sites (described in the text).

Of necessity, then, a more complicated model had to be adopted to fit the data shown in Figure 3: one that assumes two classes of sites. Data were first recast into a direct plot of the binding ratio r vs C_f (Figure 3B). The direct plot is clearly biphasic. It was deconvoluted by a curve-stripping process as follows. The initial portion of the isotherm was fit to a simple binding isotherm

$$r_1 = n_1K_1C_f/(1 + K_1C_f)$$

where K_1 is the binding constant for this class of sites and n_1 is the number of such sites. The fit to this portion of the

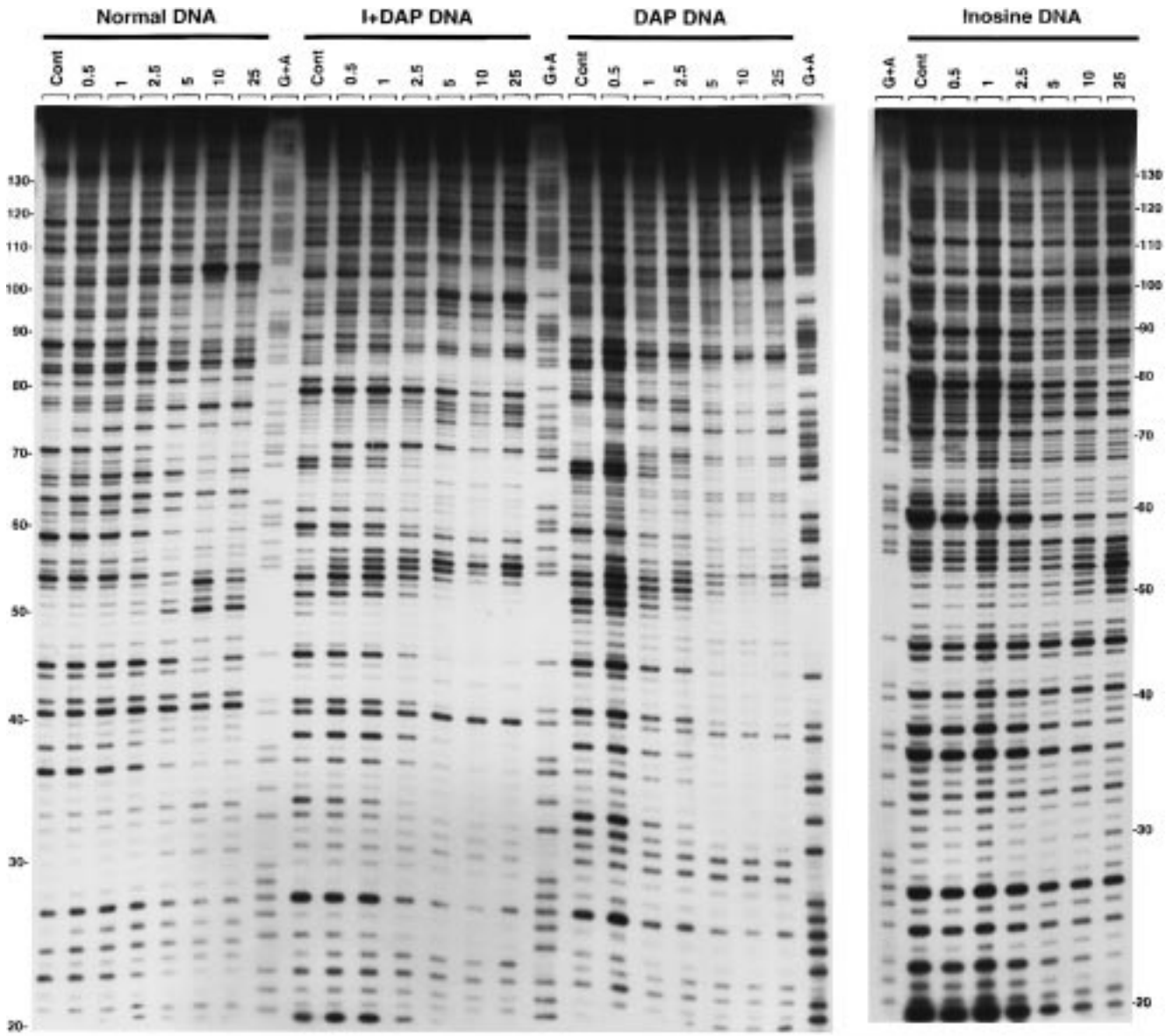

FIGURE 4: Autoradiographs showing cleavage of normal and modified DNA by DNase I in the absence (lanes marked "Cont") and presence of increasing concentrations of daunomycin (expressed as micromolar). The gel refers to the labeled Watson strand of *tyrT* DNA containing the four natural nucleotides (normal DNA), inosine residues in place of guanosine (inosine DNA), diaminopurine residues in place of adenine (DAP DNA), or inosine plus DAP residues in place of guanosine and adenine, respectively (I + DAP DNA). Chemical identities of the cleavage products were assigned by reference to formic acid−piperidine markers specific for purine residues (lanes G + A), corrected for the expected 1−1.5 band shift due to 5′ end-labeling. The scales on the sides of the autoradiographs correspond to the standard numbering of the *tyrT*(A93) sequence as represented in Figure 5.

isotherm is shown in Figure 3B as the dashed line and corresponds to $K_1 = 6.9 (\pm 0.5) \times 10^6$ M^{-1} and $n_1 = 0.078$ ($\pm$ 0.003) mol of daunomycin/mol of bp. The contribution of this class of sites was then subtracted from the remaining data, which were analyzed by a variety of binding models. The best fit to the second class of sites was obtained using the cooperative McGhee−von Hippel neighbor exclusion model (not shown), yielding the parameters $K = 5.2 (\pm 2.0) \times 10^3$ M^{-1}, $n = 5.9 (+ 2.0)$ bp, and $\omega = 106 (\pm 65)$. The composite isotherm (the sum of the individual isotherms for the two classes of sites) is shown in Figure 3B as a solid line. The minimal model to describe the data may be summarized as follows. There are two principal classes of sites for daunomycin in the fragment. A high-affinity class binds 0.08 mol of drug/mol of bp, or since the *tyrT* fragment is 160 bp long, about 13 molecules of daunomycin/DNA molecule. Following saturation of these sites, daunomycin binds weakly but with positive cooperativity to the remaining empty lattice. This class of site is eventually saturated at 0.17 mol of drug/mol of bp, or 27 daunomycin molecules/fragment in addition to the 13 already bound.

Sequence-Selective Recognition. The four different 160 base pair DNA fragments synthesized by PCR amplification were incubated with daunomycin for at least 20 min at 37 °C to establish equilibrium prior to exposing the samples to the nicking activity of DNase I. Daunomycin concentrations varying from 0.5 to 25 μM were chosen so as to generate solutions in which the fractional occupancy of DNA binding sites varied from a few percent to near 100%. Typical autoradiographs obtained with the normal and modified DNA fragments are shown in Figure 4. Visual inspection of the gels is sufficient to establish that in every case the rate of

cleavage by the enzyme is subject to considerable modulation through local binding of daunomycin.

For both strands of each DNA fragment we examined the footprinting patterns over the whole range of daunomycin concentrations so as to determine the concentration-dependence profile at defined sequences proximal and distal to the binding sites. The densitometric analyses were naturally limited to regions where the bands were sufficiently well-resolved to permit unambiguous quantification, but we obtained single-band resolution at about 100 of the 160 potential binding sites within the *tyrT* fragment on both the Watson and Crick labeled strands (from nucleotide positions 20 to 130). The corresponding differential cleavage plots in Figure 5 reveal the exact location of the footprints (negative values) as well as regions where the cleavage by the nuclease is enhanced in the presence of the antibiotic (positive values).

The plots for normal DNA (Figure 5, first pair of panels) are totally consistent with the previously published footprinting data in showing that (i) footprints generally coincide with (A/T)CG or (T/A)GC triplets (open rectangles in Figure 5); (ii) weaker footprints can also be detected at some, but not all, (A/T)C(A/T) sites (closed rectangles); and (iii) enhanced cleavage, which reflects increased accessibility of the enzyme to DNA at nonbinding sequences, is particularly strong at oligopurine·oligopyrimidine tracts such as the T_5 and T_2C_3 tracts around positions 50 and 105, respectively. With the inosine-substituted DNA, we observe that, with one exception, the footprints remain located around the canonical (A/T)CG or (T/A)GC triplets (marked by open rectangles in the illustration) but generally not at the secondary (A/T)C(A/T) sites. This implies a diminution in the ability of daunomycin to bind to the I-DNA compared to the normal DNA. Quantitative analysis of ligand-site interactions supports this conclusion. The full concentration-dependence profile for daunomycin has been determined at all binding sites in the normal and modified DNA molecules and a few examples are illustrated in Figure 6. Panels A and B in this figure show that the footprinting on natural DNA at two canonical ACG and AGC sites occurs with half-maximal effect at concentrations (C_{50}) about 1−2 μM, whereas footprinting at these two sites in inosine-substituted DNA seems to require considerably higher concentrations ($C_{50} \approx$ 10 μM). Enhancement of DNase I cutting still occurs characteristically at the A·T or I·C tracts. The situation differs from that previously reported with other DNA-intercalating antibiotics such as echinomycin and actinomycin, which failed completely to bind to inosine-containing DNA (*9*, *25*, *26*).

In the DAP-substituted DNA, all base pairs (G·C and D·T) bear a 2-amino group that obstructs access to the floor of the minor groove. However, the gels and the corresponding plots in Figure 5 reveal unambiguously that daunomycin does bind to this DNA. The 2-amino group now present on all purine nucleotides evidently does not impede the access of the drug to the base pair edges, but it does affect the recognition process since the footprinting patterns observed with DAP-containing DNA are significantly different from those obtained with normal DNA, showing that the relocation of the 2-amino group exerts a significant influence on the binding of the antibiotic. For example, the footprint at one AGC site (positions 71−73) in normal DNA in the presence of daunomycin is missing from the DAP-containing species, and conversely the footprint around position 50 in DAP DNA corresponds to a region of enhanced DNase I cleavage of the normal *tyrT* fragment. At the most sharply defined site detected in DAP-DNA, centered about the sequence 5′-CTTTDC·GTAAAG, the footprinting occurs with half-maximal effect at concentrations (C_{50}) about 1 μM (Figure 6C), suggesting that the affinity of the drug for DAP·T-containing sites in the modified DNA is about the same as its affinity for the most favored natural G·C-containing sites. Interestingly, the homopyrimidine·homopurine sequence 5′-TTTTTC·GAAAAA in normal DNA does not provide a binding site for daunomycin, whereas the corresponding DAP-containing sequence 5′-TTTTTC·GDDDDD proves to be an excellent receptor for the antibiotic (Figure 6D).

The footprinting profile observed with the doubly substituted I + DAP DNA resembles that obtained with the DNA containing DAP alone. The radically changed distribution of daunomycin binding sites in the I + DAP DNA compared to normal *tyrT* is emphasized in the differential cleavage plots of Figure 7 where the results for these two DNA species are superimposed. At many points the sites of binding (protection) and enhanced cutting are inverted in the doubly substituted polynucleotide. Just as we noted with DAP-DNA, daunomycin seems to bind surprisingly well to sequences containing a (G/C)TT triplet such as occurs at positions 48, 66, 92, and 104. The footprinting plots in Figure 6C,D further illustrate this binding characteristic.

DISCUSSION

Novel results are presented here that deepen our understanding of the binding of an important anticancer drug, daunomycin, to its preferred DNA binding sites. To the best of our knowledge, this is the first time that any drug−DNA interaction has been subjected to detailed scrutiny so as to reveal both macroscopic and microscopic drug binding events on the same DNA sequence, using a long DNA fragment produced by PCR. Moreover, the preparation of homologous fragments containing systematic base substitutions has allowed us to examine in detail the effects of DNA minor-groove substituents on daunomycin binding. The collective results provide fundamental information of potential value for the rational design of new generations of DNA binding agents.

DNase I Footprinting of Normal and Substituted tyrT DNA Fragments. Previous results showed that daunomycin binds preferentially to triplet sequences of the type 5′(A/T)GC and 5′(A/T)CG, where the notation (A/T) indicates that A or T can occupy that position (*3*, *4*, *27*). Those footprinting results were in accord with the theoretical studies of Pullman's laboratory (*28*, *29*), which correctly predicted the sequence of the preferred triplet binding site. The latest footprinting results on our biosynthetic *tyrT* fragment (Figures 4 and 5) are fully consistent with all previous daunomycin footprinting studies. The new experiments on substituted *tyrT* fragments containing inosine (for guanosine), diaminopurine (for adenine), and both inosine and diaminopurine extend the earlier observations to allow the DNA determinants of the preferential binding of daunomycin to triplet sequences to be explored. The observed effects of base substitutions on daunomycin binding to several specific sites are summarized

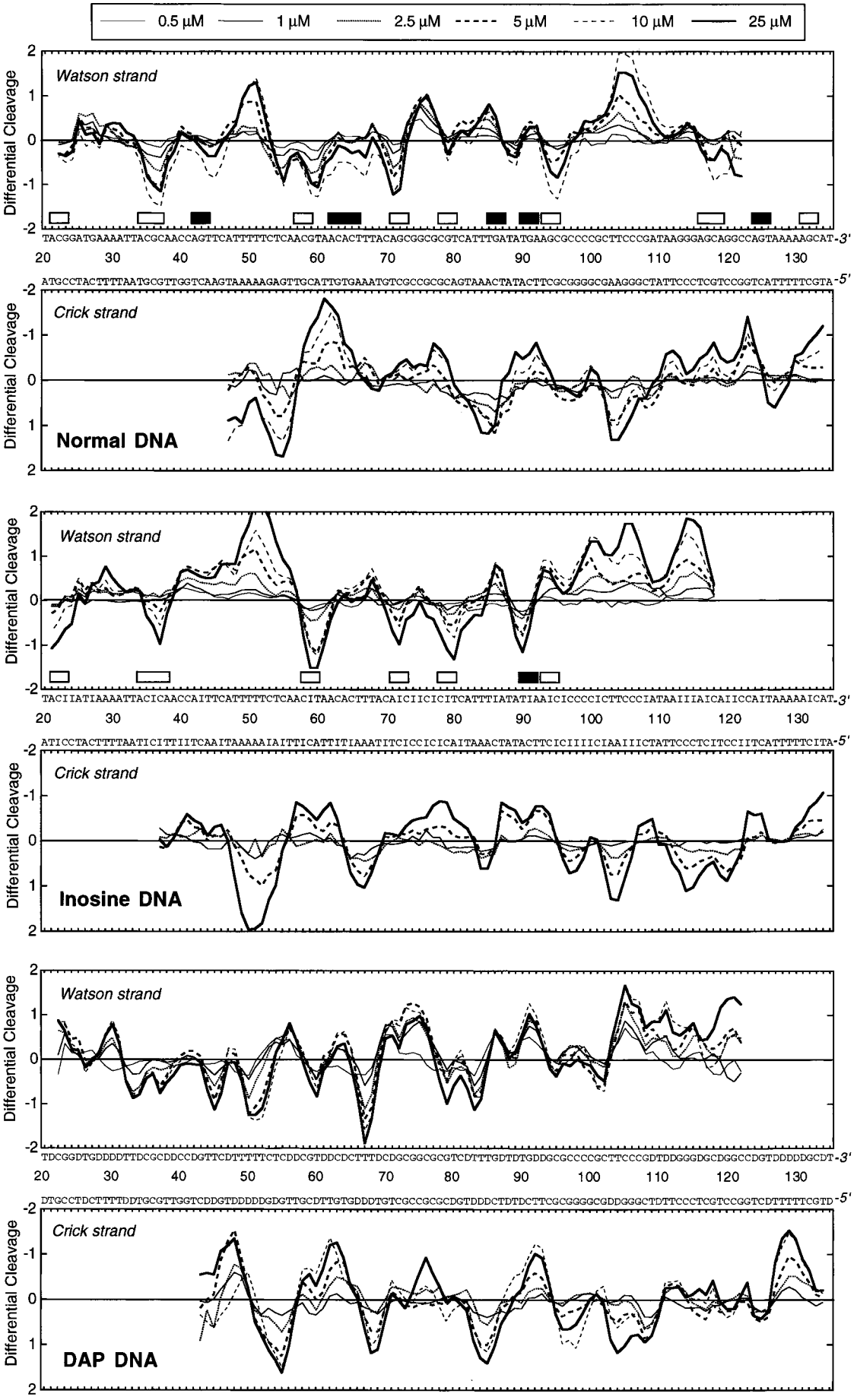
0.5 μM
1 μM
2.5 μM
5 μM
10 μM
25 μM
Watson strand
Differential Cleavage
TACGGATGAAAATTACGCAACCAGTTCATTTTTCTCAACGTAACACTTTACAGCGGCGCGTCATTTGATATGAAGCGCCCCGCTTCCCGATAAGGGAGCAGGCCAGTAAAAAGCAT-3'
20 30 40 50 60 70 80 90 100 110 120 130
ATGCCTACTTTTAATGCGTTGGTCAAGTAAAAAGAGTTGCATTGTGAAATGTCGCCGCGCAGTAAACTATACTTCGCGGGGCGAAGGGCTATTCCCTCGTCCGGTCATTTTTCGTA-5'
Crick strand
Normal DNA
Watson strand
TACIIATIAAAATTACICAACCAITTCATTTTTCTCAACITAACACTTTACAICIICICITCATTTIATATIAAICICCCCICTTCCCIATAAIIIAICAIICCAITAAAAAICAT-3'
20 30 40 50 60 70 80 90 100 110 120 130
ATICCTACTTTTAATICITTIITCAAITAAAAAIAITTICATTITIAAATITCICCICICAITAAACTATACTTCICIIIICIAAIIICTATTCCCTCITCCIITCATTTTTCITA-5'
Crick strand
Inosine DNA
Watson strand
TDCGGDTGDDDDTTDCGCDDCCDGTTCDTTTTTCTCDDCGTDDCDCTTTDCDGCGGCGCGTCDTTTGDTDTGDDGCGCCCCGCTTCCCGDTDDGGGDGCDGGCCDGTDDDDDGCDT-3'
20 30 40 50 60 70 80 90 100 110 120 130
DTGCCTDCTTTTDDTGCGTTGGTCDDGTDDDDDGDGTTGCDTTGTGDDDTGTCGCCGCGCGTDDDCTDTDCTTCGCGGGGCGDDGGGCTDTTCCCTCGTCCGGTCDTTTTTCGTD-5'
Crick strand
DAP DNA

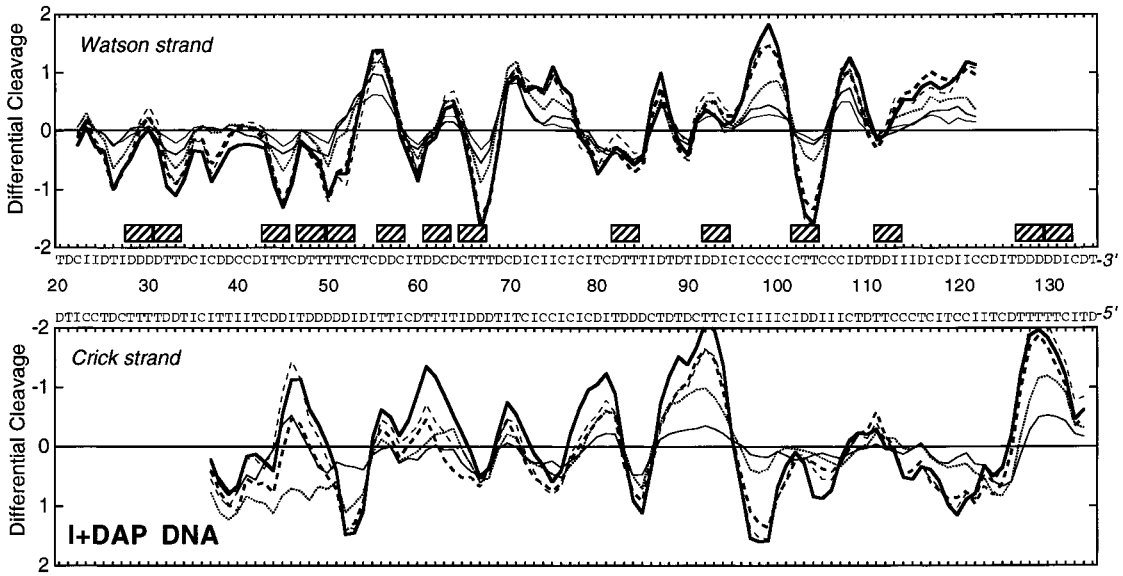

FIGURE 5: Differential cleavage plots comparing the susceptibility of the *tyrT* DNA containing normal or modified bases to cutting by DNase I in the presence of daunomycin. Antibiotic concentrations used to generate these plots were identical with those in Figure 4. The upper panel in each pair shows differential cleavage of the Watson strand; the lower panel, that of the complementary Crick strand. The ordinate scales for the two strands are inverted, so that deviation of points toward the lettered sequence (negative values) corresponds to a ligand-protected site and deviation away (positive values) represents enhanced cleavage.

in Table 1. The collective picture that emerges is that (i) the selectivity of daunomycin binding to 5′-(A/T)CG and 5′-(A/T)GC triplets is maintained with the inosine DNA, although the apparent affinity is weakened; (ii) the complete occupation of the minor groove by exocyclic amino groups on all purine residues in the DAP DNA switches the daunomycin binding preference from GC or CG sites to TD- or DT-containing sites; and (iii) the selectivity for those latter sites is maintained or even amplified in the doubly substituted I + DAP DNA. We can conclude from these observations that the 2-amino group of guanine is not absolutely necessary for the sequence-selective binding of daunomycin to 5′-(A/T)CG and 5′-(A/T)GC triplets, but it is certainly one determinant that modulates binding to preferred sites. This is most clearly evident from the finding that when we shift the purine 2-amino group from G to D nucleotides the pattern of sequence recognition by the anthracycline antibiotic is practically reversed.

We note that base substitution dramatically alters the DNase I cleavage pattern of the *tyrT* fragment. DNase I is known to cleave DNA with a modest sequence specificity (*30*). The alteration of the *tyrT* cleavage pattern upon base substitution has been rigorously and quantitatively analyzed (*5*). The changes in the cleavage pattern may be explained as resulting from the effects of base functional groups on minor-groove width and from changes in the disposition of functional groups available for interaction with DNase I upon its binding (*5*). We stress that, in the studies described here, all digestion patterns obtained in the presence of bound ligand were scrupulously referred to the correct controls of the same substituted fragment with nothing bound. In the quantitative analysis of binding, the influence of the altered cleavage pattern is therefore controlled for, leaving the differential effects resulting from the binding of the ligand clear for scrutiny.

Molecular Determinants of Daunomycin Sequence Selectivity. The molecular determinants of the preferential binding of daunomycin to the triplets 5′(A/T)GC and 5′(A/T)CG were proposed by the Pullman group (*28*, *29*) to be the 9-OH group and the daunosamine moiety. In high-resolution crystal structures the 9-OH group was observed to form a bifurcated hydrogen bond with the N-2 and N-3 substituents on the guanine base in the center of the triplet. As observed above, elimination of the N-2 substituent by substitution of inosine for guanosine does not appear to alter the binding selectivity, but it clearly diminishes the apparent affinity for particular sites (see Figure 6A). Interaction of the 9-OH group with the N-3 substituent is presumably still possible following the G to I substitution. Recent studies on the effect of altering key daunomycin substituents on binding energetics (*31*) complement and confirm the effect of N-2 elimination described here. The binding free energy for 9-deoxydoxorubicin (a compound that lacks the 9-OH group of the drug) was found to be 1.1 kcal mol^{-1} *less* favorable than DG for the parent compound, doxorubicin. Such a change in free energy corresponds to about a 10-fold *decrease* in the binding constant, which is in excellent agreement with the magnitude of the effect seen the footprinting titration experiment shown in Figure 6A. Substitution of inosine for guanosine leads to loss of the same key hydrogen-bonding opportunity as does elimination of the 9-OH group on daunomycin. The observed and reported effects are complementary and mutually consistent.

The preference for an A·T base pair at the 5′ end of the target triplet was considered to arise from a steric effect. Proper fitting of the daunosamine moiety into the minor groove would be hindered by the bulky N-2 substituent of guanine if a G·C base pair were to occupy that position in the triplet sequence. Daunosamine contributes over 2 kcal mol^{-1} to the overall DNA binding affinity of daunomycin (*31*). The results of inosine and diaminopurine substitution may be rationalized against this background. No particular shift in sequence binding preference occurs upon inosine substitution alone. However, full substitution (I for G and

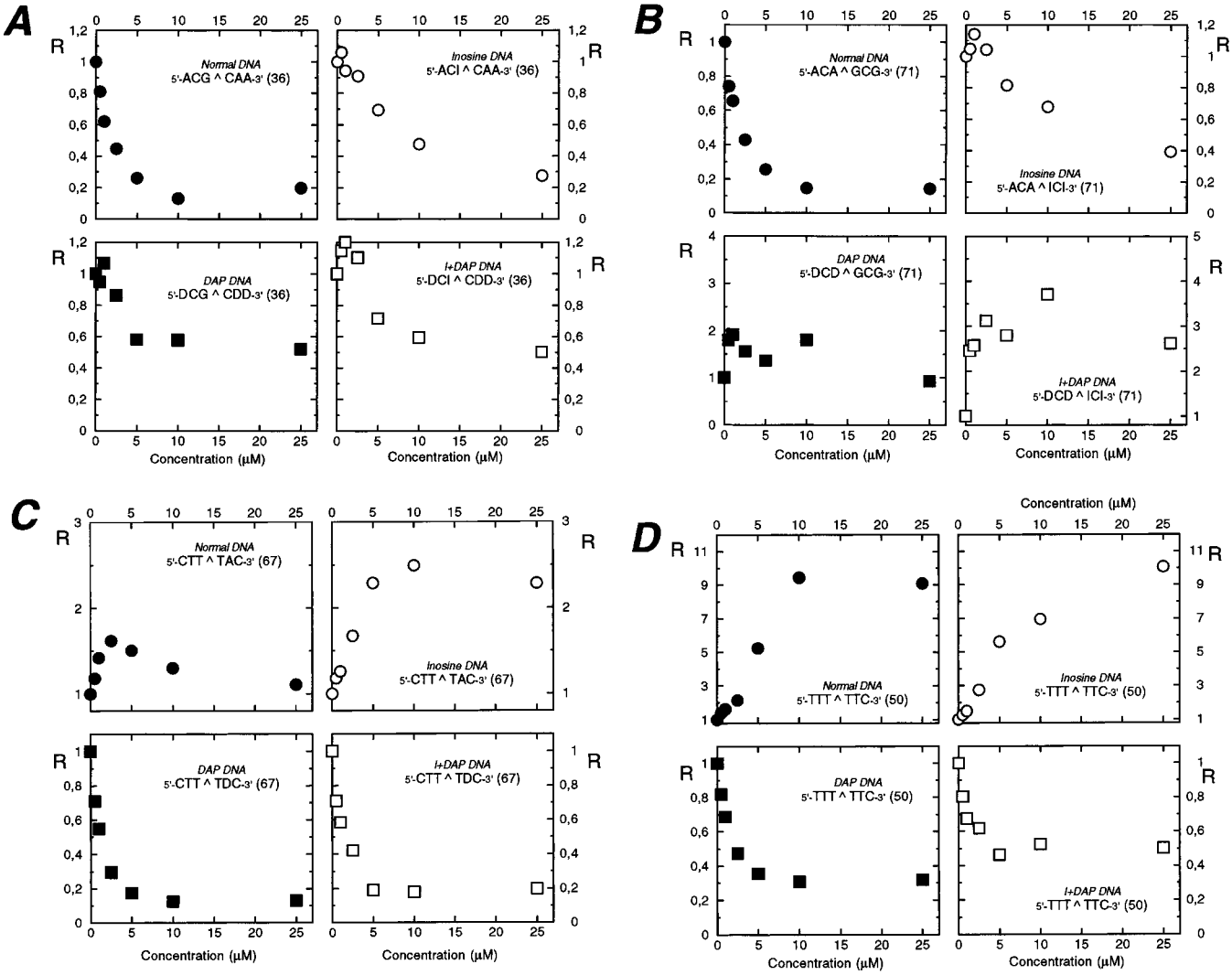

FIGURE 6: Footprinting plots for selected bonds in the *tyrT* sequences. The relative band intensity R corresponds to the ratio I_c/I_0, where I_c is the intensity of the band at the ligand concentration c and I_0 is the intensity of the same band in the absence of the antibiotic. Data points were obtained from gels such as the ones shown in Figure 4.

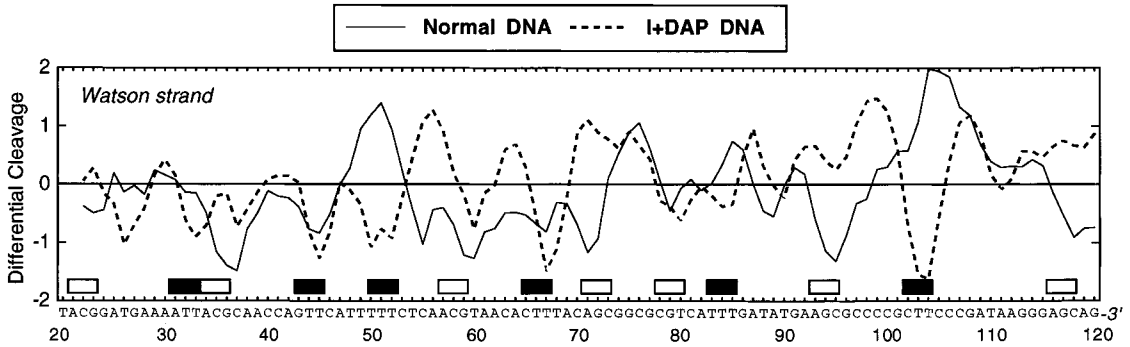

FIGURE 7: Differential cleavage plots comparing the DNase I-mediated cleavage of normal and I + DAP-containing DNA in the presence of 10 μM daunomycin. The plot drawn as a dashed line refers to the modified DNA fragment containing inosine and DAP residues, and the plot indicated by a continuous line refers to normal DNA. Open boxes mark the position of (A/T)CG or (A/T)GC sites; closed boxes refer to XTT sites. Other details are as for Figure 5.

D for A) produces a dramatic shift in the distribution of protected sequences (see Figure 7). The best footprints in the I + DAP DNA appear to occur in the vicinity of triplets composed of adjacent DAP·T base pairs flanked by an I·C base pair. Such a result is exactly what would be expected if the steric hindrance proposal is correct. The interpretation would be, in such cases, that the anthraquinone ring intercalates between the two DAP·T base pairs, leaving the daunosamine extending down the minor groove where it covers the I·C base pair.

Simultaneous Macroscopic and Microscopic Binding Studies. The availability of reasonably large quantities of homogeneous *tyrT* DNA prepared by PCR has allowed us, for the first time, to examine both the *macroscopic* binding of daunomycin by fluorescence titration and *microscopic* binding events by DNase I footprinting. The results of these

Table 1: Response of Specific Sites to Daunomycin in Normal and Substituted *tyrT* DNA

position	sequence	normal DNA	inosine DNA	DAP DNA	I + DAP DNA
36	5′-ACG^{I}CAA-3′	protected (2 μM)	protected (10 μM)	protected (5−25 μM)	protected (10−25 μM)
45	5′-GTT^{I}CAT-3′	protected (>25 μM)	enhanced	protected (3 μM)	protected (2 μM)
59	5′-ACG^{I}TAA-3′	protected (2 μM)	protected (2 μM)	protected (2.5 μM)	protected (10−25 μM)
71	5′-ACG^{I}CAA-3′	protected (2.5 μM)	protected (20 μM)	unchanged	enhanced
95	5′-AGC^{I}GCC-3′	protected (5 μM)	enhanced	protected (>25 μM)	unchanged
33	5′-ATT^{I}ACG-3′	unchanged	unchanged	protected (1.5 μM)	protected (1 μM)
64	5′-ATT^{I}ACG-3′	unchanged	enhanced	enhanced	enhanced
90	5′-TAT^{I}GAT-3′	unchanged	protected (5 μM)	enhanced	unchanged
26	5′-TAT^{I}GAT-3′	enhanced	enhanced	unchanged	protected (>25 μM)
50	5′-TTT^{I}TTC-3′	enhanced	enhanced	protected (2 μM)	protected (5−25 μM)
67	5′-CTT^{I}TAC-3′	enhanced	enhanced	protected (1.5 μM)	protected (1.5 μM)
77	5′-GCG^{I}CGT-3′	enhanced	unchanged	enhanced	unchanged
85	5′-TTT^{I}GAT-3′	enhanced	enhanced	unchanged	protected
103	5′-TCG^{I}TCC-3′	enhanced	enhanced	unchanged	protected (2.5 μM)
106	5′-TCC^{I}CGA-3′	enhanced	enhanced	unchanged	protected (>25 μM)

investigations reveal much about how daunomycin binds to a DNA lattice. Historically, drug binding to DNA has been analyzed by neighbor exclusion models (*24*, *31*). The data obtained here show conclusively that assumptions which are fundamental to the neighbor exclusion model are violated and that more complex models are needed to analyze the daunomycin binding isotherm properly. Footprinting reveals a class of high-affinity sites that are occupied before any neighbor exclusion effects would influence binding. Presumably these sites would be the ones preferentially filled by daunomycin in vivo, where DNA is likely to be in large excess of drug.

The neighbor exclusion model cannot describe the binding of daunomycin to the *tyrT* fragment (Figure 3A) even if more complicated variants that include negative cooperativity are used. All such models assume that the DNA lattice is comprised of identical binding sites of equal affinity, an assumption that DNase I footprinting demonstrates unequivocally to be incorrect (Figure 6). By using a homogeneous, PCR synthesized DNA preparation for macroscopic binding measurements, the heterogeneity of binding sites is clearly revealed (Figure 3B). Such heterogeneity is fully consistent with the microscopic binding events revealed by footprinting, where some sites are seen not to bind daunomycin at all, while those that do bind the drug do so with a distribution of affinities (Figure 6) (*2*). We find from our analysis of macroscopic binding data that there are approximately 13 high-affinity sites for daunomycin within the *tyrT* sequence, characterized by an association constant of 6.9×10^6 M^{-1} in 0.2 M NaCl. We note that this binding constant is fully an order of magnitude larger than the macroscopic binding constant determined for daunomycin with calf thymus DNA under the same solution conditions (*2*). Moreover, footprinting has revealed that daunomycin binds preferentially to triplet sequences of the type 5′(A/T)GC or 5′ (A/T)CG. A total of 16 sites conforming to that general motif can be identified in the *tyrT* sequence. The near equivalence between the number of high-affinity sites and the number of preferred triplets leads us to believe that the binding constant 6.9×10^6 M^{-1} refers to the interaction of daunomycin with such sites.

Weaker, cooperative binding of daunomycin to the *tyrT* lattice following saturation of high-affinity sites is also consistent with the results obtained from quantitative footprinting experiments. Footprinting at certain sequences shows complicated, sigmoidal titration curves (*4*), consistent with positive cooperativity in the binding of the ligand. The origin of such cooperativity is at present unclear. A plausible explanation would be that it arises from coupling of binding at such sequences to conformational transitions in the *tyrT* lattice resulting from occupancy of the high-affinity sites.

Daunomycin Binding to A Tracts. In the normal *tyrT* fragment, daunomycin neither binds to nor protects sequences containing an oligomeric nonalternating A tract (Figure 5, first pair of panels, positions 30, 50, and 128). Indeed, there is enhanced cleavage around these sequences in the presence of daunomycin, perhaps resulting from conformational changes in the DNA. Previous studies (*33*) have shown that daunomycin binds only weakly and cooperatively to poly (dA)·poly (dT). Its binding results in allosteric effects, among which is an enhanced susceptibility to cleavage by DNase I (*33*). The evident binding of daunomycin at or close to certain sequences that were A tracts upon substitution with diaminopurine is a striking result. Apart from the possible hydrogen-bonding opportunity involving the N-2 amino group in diaminopurine, it is conceivable that some structural effects could contribute to promote binding as well. The width of the minor groove is known to increase in diaminopurine-substituted A tracts (*5*), perhaps facilitating intercalation of the anthracycline chromophore.

It is quite unusual for an intercalating agent to bind preferentially to nonalternating oligoT·oligoD sequences (see

the strong footprints around positions 50, 67, and 130 in Figure 5, fourth pair of panels). A search for the common denominator of the new binding sites for daunomycin suggests that the drug may be selective for TT·DD dinucleotide steps, with a preference for YTT (i.e., TTT and CTT) compared to RTT (DTT and GTT) triplets. We can postulate that the drug intercalates its anthraquinone chromophore between the two juxtaposed Ts, allowing the C-9 hydroxyl group of the D ring to contact the N-3 and/or the exocyclic N-2 of one the diaminopurine bases, leaving the daunosamine located within the minor groove covering the adjacent I·C pair. Interestingly, it can be seen that in most cases the intensity of the footprint around 5′-CTT·DDG or 5′-GTT·DDC sequences in the DAP-DNA becomes more pronounced when the G residue is replace with an I (for example, compare the weak footprint at the 5′-CTT site at position 103 in Figure 5, third pair of panels, with the intense footprint at the same site in Figure 5, fourth pair of panels). It is logical to suggest that the removal of the 2-amino group from the G·C base pair favors fitting of the carbohydrate domain of the drug into the minor groove at the triplet binding site. A similar explanation has been proposed previously to explain tighter binding of daunomycin to (A/T)GC trinucleotides compared to (G/C)GC triplets in normal DNA. However, the reason daunomycin should intercalate preferentially between two consecutive D·T pairs remains to be elucidated. In that regard, it is important to mention that for daunomycin, as previously observed with actinomycin, the concentration range over which strong footprints develop with the DAP-containing DNA is not much different from that seen with natural DNA, whereas for an antibiotic such as echinomycin there is at least an order of magnitude increase in sensitivity (*34*). Careful comparison of drug and base pair dipole moments, as undertaken by Gallego et al. (*35*−*37*), might prove informative.

SUMMARY AND CONCLUSIONS

PCR was used to synthesize homologous *tyrT* DNA fragments that differed in the disposition of substituents in the minor groove. Loss of the N-2 of guanine had little effect on the sequence preference of daunomycin binding, although binding to preferred sites appeared to be weaker. All the signs are that these effects can be attributed to a hydrogen-bonding interaction between the 9-OH group on daunomycin and the N-2 of guanine. Reversal of the disposition of the N-2 amino group by substitution of inosine for guanosine and diaminopurine for adenine completely reversed the sequence preference of daunomycin. In the doubly substituted fragment, preferred binding occurs at the triplet motif 5′IDD, in contrast to the preferred 5′(A/T)GC and 5′(A/T)-CG triplets in the normal, unsubstituted fragment. This switch may be attributed to the aversion of the daunosamine moiety for the N-2 group in the minor groove, the presence of which produces a steric clash with the carbohydrate. Detailed comparison of all results using the substituted fragments provides a critical test of the proposed molecular determinants of DNA recognition by daunomycin and confirms the key roles of the 9-OH group and the daunosamine. Simultaneous macroscopic and microscopic binding studies show that daunomycin binding to the *tyrT* fragment is complex and that multiple classes of binding sites of differing affinity must be considered to account quantitatively for the observed binding isotherms. A class of binding sites with high affinity (10^7 M^{-1}), most probably corresponding to the 5′(A/T)GC and 5′ (A/T)CG triplets, was identified and characterized. It is clear from the footprinting work that the fundamental assumptions of neighbor exclusion models are violated, and that such models offer an oversimplified description of the binding process in the present case, which is unlikely to be atypical among drug−DNA interactions at large.

SUPPORTING INFORMATION AVAILABLE

Figure S1, showing CD and UV difference spectra for normal and substituted *tyrT* fragments (1 page). Ordering information is given on any current masthead page.

REFERENCES

1. Chabner, B. A., and Longo, D. L. (1996) *Cancer chemotherapy and biotherapy. Principles and practice*, 2nd ed., Lippincott-Raven Publishers, New York.
2. Chaires, J. B. (1996) in *Advances in DNA Sequence Specific Agents* (Hurley, L. H., and Chaires, J. B., Eds.) Vol. 2, pp 141−167, JAI Press, Greenwich, CT.
3. Chaires, J. B., Fox, K. R., Herrera, J. E., Britt, M., and Waring, M. J. (1987) *Biochemistry 26*, 8227−8236.
4. Chaires, J. B., Herrera, J. E., and Waring, M. J. (1990) *Biochemistry 29*, 6145−6153.
5. Bailly, C., Mollegaard, N. E., Nielsen, P. E., and Waring, M. J. (1995) *EMBO J. 14*, 2121−2131.
6. Jen-Jacobsen, L. (1995) *Methods Enzymol. 259*, 305−344.
7. Aiken, C. R., and Gumport, R. I (1991) *Methods Enzymol. 208*, 433−457.
8. Drew, H. R., Weeks, J. R., and Travers, A. A. (1985) *EMBO J. 4*, 1025−1032.
9. Marchand, C., Bailly, C., McLean, M. J., Moroney, S. E., and Waring, M. J. (1992) *Nucleic Acids Res. 20*, 5601−5606.
10. Sayers, E. W., and Waring, M. J. (1993) *Biochemistry 32*, 9094−9107.
11. Bloch, W. (1991) *Biochemistry 30*, 2735−2747.
12. Maniatis, T., Fritsch, E. F., and Sambrook, J. (1982) *Molecular Cloning: A Laboratory Manual*, Cold Spring Harbor Laboratory Press, Cold Spring Harbor, NY.
13. Bailly, C., and Waring, M. J. (1995) *J. Biomol. Struct. Dyn. 12*, 869−898.
14. Johnston, R. F., Pickett, S. C., and Barker, D. L. (1990) *Electrophoresis 11*, 355−360.
15. Ward, B., Rehfuss, R., and Dabrowiak, J. C. (1987) *J. Biomol. Struct. Dyn. 4*, 685−695.
16. Dabrowiak, J. C., and Goodisman, J. (1989) in *Chemistry and Physics of DNA−Ligand Interactions* (Kallenbach, N. R., Ed.) pp 143−174, Adenine Press, Guilderland, NY.
17. Dabrowiak, J. C., Kissinger, K., and Goodisman, J. (1989) *Electrophoresis 10*, 404−412.
18. Stankus, A., Goodisman, J., and Dabrowiak, J. C. (1992) *Biochemistry 31*, 9310−9318.
19. Shubsda, M., Kishikawa, H., Goodisman, J., and Dabrowiak, J. (1994) *J. Mol. Recog. 7*, 133−139.
20. Bailly, C., Hamy, F., and Waring, M. J. (1995) *Biochemistry 35*, 1150−1161.
21. Correia, J. J., and Chaires, J. B. (1994) in *Methods in Enzymology* (Brand, L., and Johnson, M. L., Eds.) Vol. 240, pp 593−614, Academic Press, Inc., San Diego, CA.
22. Hirschman, S. Z., and Felsenfeld, G. (1966) *J. Mol. Biol. 16*, 347−358.
23. Waring, M. J., and Bailly, C. (1994a*) J. Mol. Recog. 7*, 109−122.
24. McGhee, J. D., and von Hippel, P. H. (1974) *J. Mol. Biol. 86*, 469−489.
25. Waring, M. J., and Bailly, C. (1994*) Gene 149*, 69−79.
26. Jennewein, S., and Waring, M. J. (1997) *Nucleic Acids Res. 25*, 1502−1509.

27. Chaires, J. B. (1995) in *Anthracycline Antibiotics: New Analogues, Methods of Delivery, and Mechanisms of Action* (Priebe, W., Ed) ACS Symposium Series 574, pp 155−167, American Chemical Society, Washington, DC.
28. Chen, K.-X., Gresh, N., and Pullman, B. (1985) *J. Biomol. Struct. Dynam. 3*, 445−466.
29. Pullman, B. (1990) *Anti-Cancer Drug Des. 7*, 95−105.
30. Herrera, J. E., and Chaires, J. B. (1994) *J. Mol. Biol. 236*, 405−411.
31. Chaires, J. B., Satyanarayana, S., Suh, D., Fokt, I. Przewloka, T., and Priebe, W. (1996) *Biochemistry 35*, 2047−2053.
32. Crothers, D. M. (1968) *Biopolymers 6*, 575−584.
33. Herrera, J. E., and Chaires, J. B. (1989) *Biochemistry 28*, 1993−2000.
34. Bailly, C., Marchand, C., and Waring, M. J. (1993) *J. Am. Chem. Soc. 115*, 3784−3785.
35. Gallego, J., Luque, F. J., Orozco, M., Burgos, C., Alvarez-Builla, J., Rodrigo, M. M., and Gago, F. (1994) *J. Med. Chem. 37*, 1601−1609.
36. Gallego, J., de Pascual-Teresa, B., Ortiz, A. R., Pisabarro, M. T., and Gago, F. (1995) in *QSAR and Molecular Modeling: Concepts, Computational Tools and Biological Applications* (Sanz, F., Giraldo, J., and Manaut, F., Eds.) pp 274−281, Prous Science Publishers, Barcelona, Spain.
37. Gallego, J., Ortiz, A. R., de Pascual-Teresa, B., and Gago, F. (1997) *J. Comput.-Aided Mol. Des. 11*, 114−128.

BI9716128